Architecture of the cerebral cortical association connectome underlying cognition

Mihail Bota[a,1], Olaf Sporns[b], and Larry W. Swanson[a,2]

[a]Department of Biological Sciences, University of Southern California, Los Angeles, CA 90089; and [b]Department of Psychological and Brain Sciences, Indiana University, Bloomington, IN 47405

Contributed by Larry W. Swanson, March 9, 2015 (sent for review January 13, 2015; reviewed by Fred H. Gage and Marcus E. Raichle)

Cognition presumably emerges from neural activity in the network of association connections between cortical regions that is modulated by inputs from sensory and state systems and directs voluntary behavior by outputs to the motor system. To reveal global architectural features of the cortical association connectome, network analysis was performed on >16,000 reports of histologically defined axonal connections between cortical regions in rat. The network analysis reveals an organization into four asymmetrically interconnected modules involving the entire cortex in a topographic and topologic core–shell arrangement. There is also a topographically continuous U-shaped band of cortical areas that are highly connected with each other as well as with the rest of the cortex extending through all four modules, with the temporal pole of this band (entorhinal area) having the most cortical association connections of all. These results provide a starting point for compiling a mammalian nervous system connectome that could ultimately reveal novel correlations between genome-wide association studies and connectome-wide association studies, leading to new insights into the cellular architecture supporting cognition.

cerebral cortex | connectomics | mammal | network analysis | neural connections

The cerebral cortex is the core of the brain's cognitive system (1, 2). Emerging evidence suggests that misdirected and/or dysfunctional cortical connections established during neurodevelopment, or degenerative events later in life, are fundamental to cognitive alterations associated with brain disorders like Alzheimer's disease, autism spectrum disorder, and schizophrenia (3). Presumably, an understanding of biological mechanisms underlying cognition and the control of voluntary behavior rests at least partly on the structure–function wiring diagram of the cortex. Design principles of this neural circuitry are based on a network of interactions between distributed nervous system regions, and on the underlying function of their constituent neuron populations, and individual neurons.

Unfortunately, a global structure–function wiring diagram of the cortex has not yet been elaborated (4). A necessary, but not sufficient, prerequisite for establishing this basic plan is a comprehensive structural model of cortical connectivity (5–7). Such a "roadmap" could then be used as a database scaffolding for molecular, cellular, physiological, behavioral, and cognitive data and for modeling (8)—analogous to a Google Maps for the brain. The research strategy described here provides the starting point for such a model, as well as a framework, benchmark, and infrastructure for developing a global account of nervous system structural network organization as a whole.

The conceptual framework underlying our strategy to analyze global nervous system connection architecture is twofold. First, because of considerable complexity—for example, human isocortex on one side has 6–9 billion neurons (9–11) interconnected by orders-of-magnitude-more synapses—three hierarchical (nested) levels analysis are considered (12, 13). A macroconnection between two gray-matter regions considered as black boxes is at the top of the hierarchy, a mesoconnection between two neuron types (14) within or between regions is nested within a macroconnection, and a microconnection between two individual neurons anywhere in the nervous system is nested within a mesoconnection. Second, small mammals, instead of humans, are analyzed. Data are generated much more quickly from small brains, and experimental pathway tracing of human axonal connections is currently impermissible.

MR diffusion tractography offers exciting new approaches to identifying human cortical connections, but inherent resolution limits require correlation and validation with experimental histological pathway tracing data in animals. Tractography deals only with white-matter organization, not the cellular origin and synaptic termination of connections in gray matter, and the method cannot identify unambiguously the directionality (from–to relations) of identified tracts or distinguish histologically defined gray-matter regions themselves. Historically, similar limitations applied to the gross anatomical methods used to discover human regionalization and cortical association tracts almost 150 y ago (15).

Because the richest current experimental histological data on intracortical connectivity are for adult rat, this peer-reviewed neuroanatomical literature was systematically and expertly curated for network analysis. One goal was to begin by establishing a general plan for mammalian cortical association connections

Significance

Connections between cerebral cortex regions are known as association connections, and neural activity in the network formed by these connections is thought to generate cognition. Network analysis of microscopic association connection data produced over the last 40 years in a small, easily studied mammal suggests a new way to describe the organization of the cortical association network. Basically, it consists of four modules with an anatomical shell–core arrangement and asymmetric connections within and between modules, implying at least partly "hardwired," genetically determined biases of information flow through the cortical association network. The results advance the goal of achieving a global nervous system wiring diagram of connections and provide another step toward understanding the cellular architecture and mechanisms underpinning cognition.

Author contributions: M.B. and L.W.S. designed research; M.B. performed research; M.B. and O.S. analyzed data; and L.W.S. wrote the paper.

Reviewers: F.H.G., The Salk Institute for Biological Studies; and M.E.R., Washington University in St. Louis.

The authors declare no conflict of interest.

Data deposition: The connectional data are available online at the Brain Architecture Knowledge Management System (BAMS; brancusi1.usc.edu/connections/grid/168); network analysis tools are available at the Brain Connectivity Toolbox (www.brain-connectivity-toolbox.net).

[1]Present address: International Neuroinformatics Coordinating Facility, University of California at San Diego, La Jolla, CA 92093.

[2]To whom correspondence should be addressed. Email: lswanson@usc.edu.

This article contains supporting information online at www.pnas.org/lookup/suppl/doi:10.1073/pnas.1504394112/-/DCSupplemental.

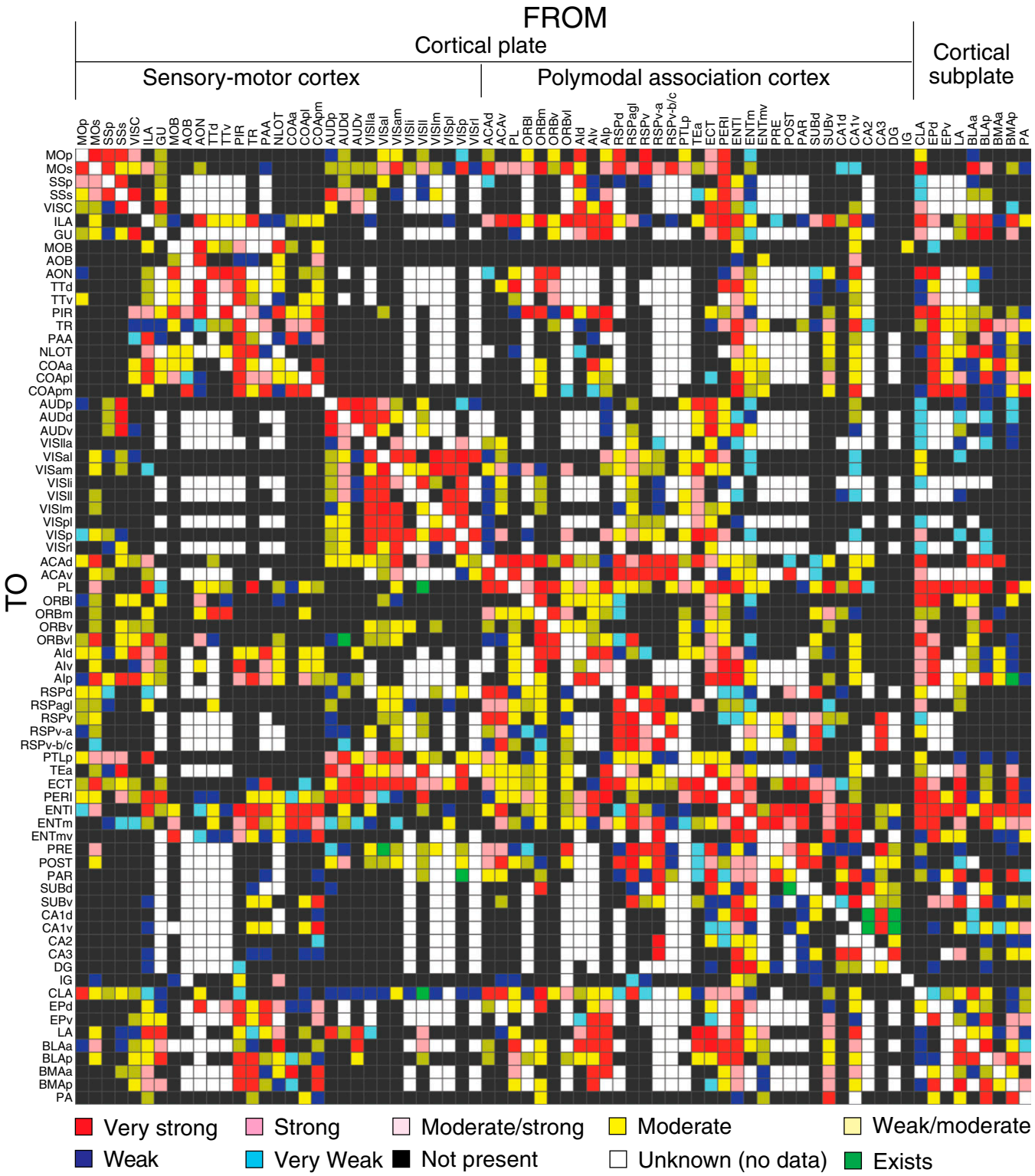

Fig. 1. Rat cortical association connectome. Directed synaptic macroconnection matrix with gray-matter region sequence (top left to right, list of macroconnection origins, from; left side top to bottom, same list of macroconnection terminations, to) in the Swanson-04 (16) structure–function nomenclature hierarchy. The main diagonal (top left to bottom right) is empty because connections within a region are not considered in the analysis. Color scale of connection weight is at bottom; abbreviations are in Fig. S2.

(4): excitatory (glutamatergic) connections established between cortical regions in one hemisphere by pyramidal neurons, as opposed to commissural connections between right and left hemispheres (a logical next step, followed by axonal inputs and outputs of the cortex). The other goal was to propose a comprehensive and systematic correlative bridge between data from experimental pathway tracing in animals and diffusion tractography in humans.

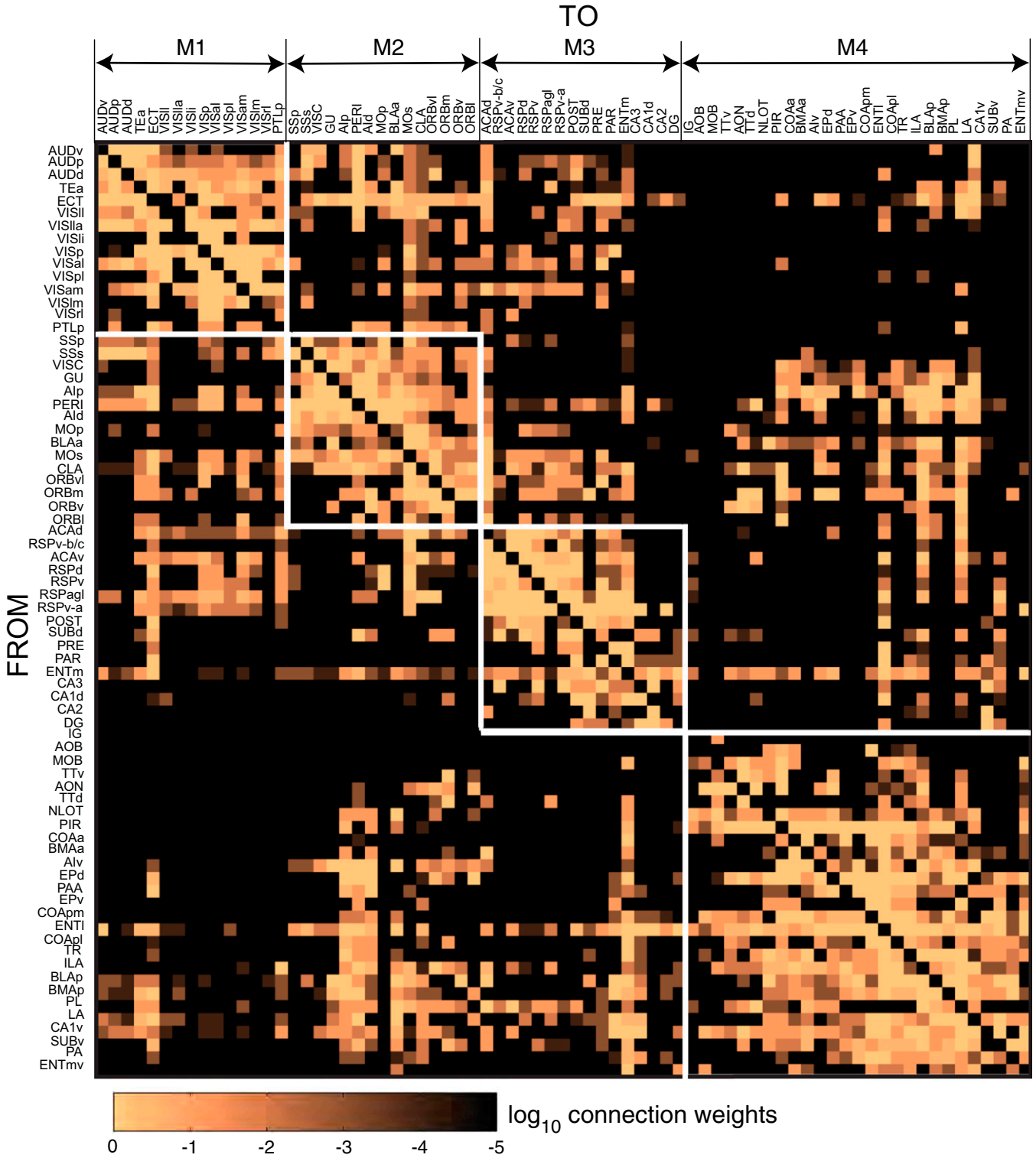

Fig. 2. Four modules of rat cortical association network (M1–M4). Directed synaptic macroconnections are arranged here by connection weight, rather than by nomenclature hierarchy (Fig. 1). The matrix (log-weighted scaled connection weighs, bottom) shows four highly interconnected modules (inside white boxes along main diagonal) that together include all 73 regions in the analysis, with intermodular connections shown outside the boxes. "Not present" and "unknown" are black; abbreviations are in Fig. S2.

Results

Cortical Association Connection Number. Systematic curation of the primary neuroanatomical literature yielded 1,923 rat cortical association macroconnections (RCAMs) as present (242, or 12.6% from the L.W.S. laboratory) and 2,341 as not present (of those possible, 45.1% present, indicating a very highly connected network)—between the 73 gray-matter regions analyzed for the cerebral cortex as a whole. No adequate published data were

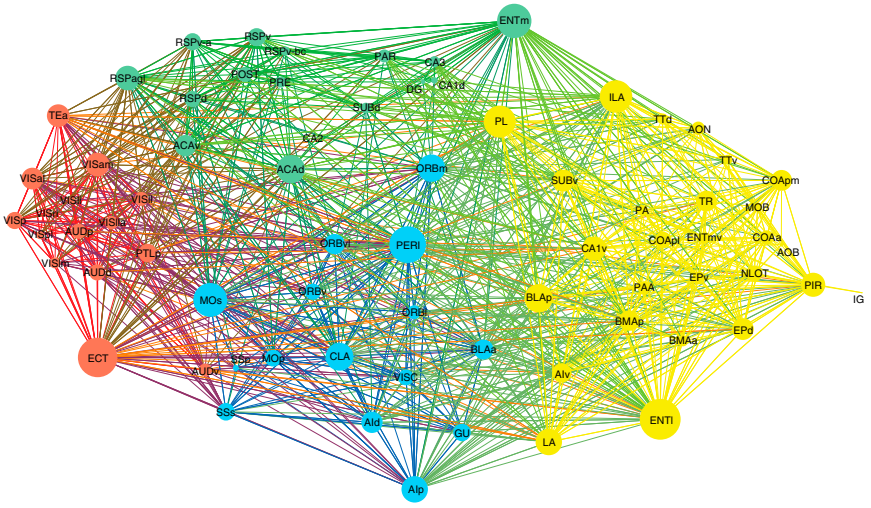

Fig. 3. Circuit diagram constructed using Gephi's weighted 3D force-directed algorithm. Node color indicates module number (M1, red; M2, blue; M3, green; M4, yellow), with size proportional to node degree (Fig. S1*C*). Edge color indicates output of correspondingly colored node; edge thickness is proportional to connection weight. "Very weak" and "weak" weights were dropped from analysis, minimizing the influence of false-positive results. Abbreviations are in Fig. S2.

found for 992 (18.9%) of all 5,256 ($73^2 - 73$) possible macroconnections. Assuming the curated literature representatively samples the 73-region matrix, the complete RCAM dataset would contain ~2,370 macroconnections (5,256 × 0.451), with a remarkably high average of 32 output association macroconnections per cortical region (2,370/73). However, RCAM number varied greatly for particular cortical regions (input range 9–51, output range 1–57). The dataset was derived from >16,000 RCAM connection reports, publicly available in the Brain Architecture Knowledge Management System (BAMS), expertly curated from >250 references in the primary literature.

Network Analysis for Modules. The RCAM dataset was first displayed in matrix format with column and row ordering following the cortical region sequence in the hierarchical structure–function nomenclature of Swanson-04 (16). Fig. 1 is a connection lookup table (matrix) automatically generated in BAMS2 Workspace (17) and provides a visual overview of connections that are reportedly present, are not present, or remain unexamined. Each of the 73 histologically defined cortical regions displays a unique set of input and output association connections with other cortical regions on the same side of the brain.

Modularity analyses (18) of the RCAM dataset that optimize a metric based on connection weights (Fig. S1 *A* and *B*) showed in connection matrix form (Fig. 2) that all 73 cortical regions cluster in one of four distinct modules (M1–M4) arranged in the matrix, such that more strongly connected modules are adjacent, and within-module regions more strongly connected are also adjacent (Fig. 2; Fig. S2 lists the 73 components with their abbreviations). This result was confirmed by using an alternate, circuit diagram graph analysis approach based on a force-directed algorithm (Fig. 3).

To distinguish visually whether module components are anatomically either interdigitated or segregated, they were mapped onto a topologically accurate cortical flatmap (16). Clearly, each module is a spatially continuous domain, with the four modules together covering the entire cortical mantle in a shell and core arrangement (Fig. 4*A*). This basic arrangement is also seen, although less clearly, in more familiar surface and cross-sectional views of the cortex (Fig. 5), and it is revealed in yet another view—all 1,923 association connections mapped onto the flatmap (Fig. 6).

Two modules form a complete shell (ring) around the medial edge of the cerebral cortex—roughly corresponding to the limbic region (lobe)—whereas the other two modules form a core within the shell—roughly corresponding to the cerebral hemisphere's lateral convexity. The caudal core (hemispheric) module (M1) contains visual and auditory areas and related association areas including posterior parietal and dorsal and ventral temporal. The rostral core (hemispheric) module (M2) contains somatic and visceral sensory–motor and gustatory areas and related association areas including orbital, agranular insular, and perirhinal. The dorsal shell (limbic) module (M3) contains the anterior cingulate and retrosplenial areas and major parts of the hippocampal formation, including medial entorhinal area, parasubiculum, presubiculum, postsubiculum, dorsal subiculum and dorsal field CA1, field CA3, and dentate gyrus. The ventral shell (limbic) module (M4) contains the most components, primarily regions belonging to the olfactory system, infralimbic and prelimbic areas (of the so-called medial prefrontal cortex), lateral amygdalar nucleus, and some hippocampal formation parts (lateral entorhinal area, ventral subiculum, and ventral field CA1).

Small World, Hubs, and Rich Club. Weighted network analysis of the RCAM dataset revealed two important hallmarks of local and global network organization—high clustering and high global efficiency, respectively. A high clustering value ($C = 0.084$), exceeding that found in a null model comprising a population of randomized networks ($C_{rand} = 0.057 \pm 6 \times 10^{-4}$, mean and SD for 10,000 randomized controls), indicates that if two cortical regions (nodes) are mutually connected, then it is highly probable (and more likely than expected by chance) that they also have common network neighbors. Such high clustering suggests that mutually connected regions have similar connectivity profiles as commonly found in local network clusters. The value of RCAM dataset's global efficiency ($G = 0.352$) is high and very close to those found in a population of randomized controls ($G_{rand} = 0.379 \pm 0.002$), indicating that the shortest paths between any two regions tend to comprise only a small number of steps, thus enabling effective global communication across the network. Together, high clustering and high efficiency (short path length) have been recognized as the defining features of small-world networks (19).

As in other connectome analyses, network measures allow us to identify nodes (here cortical regions) that are more strongly or

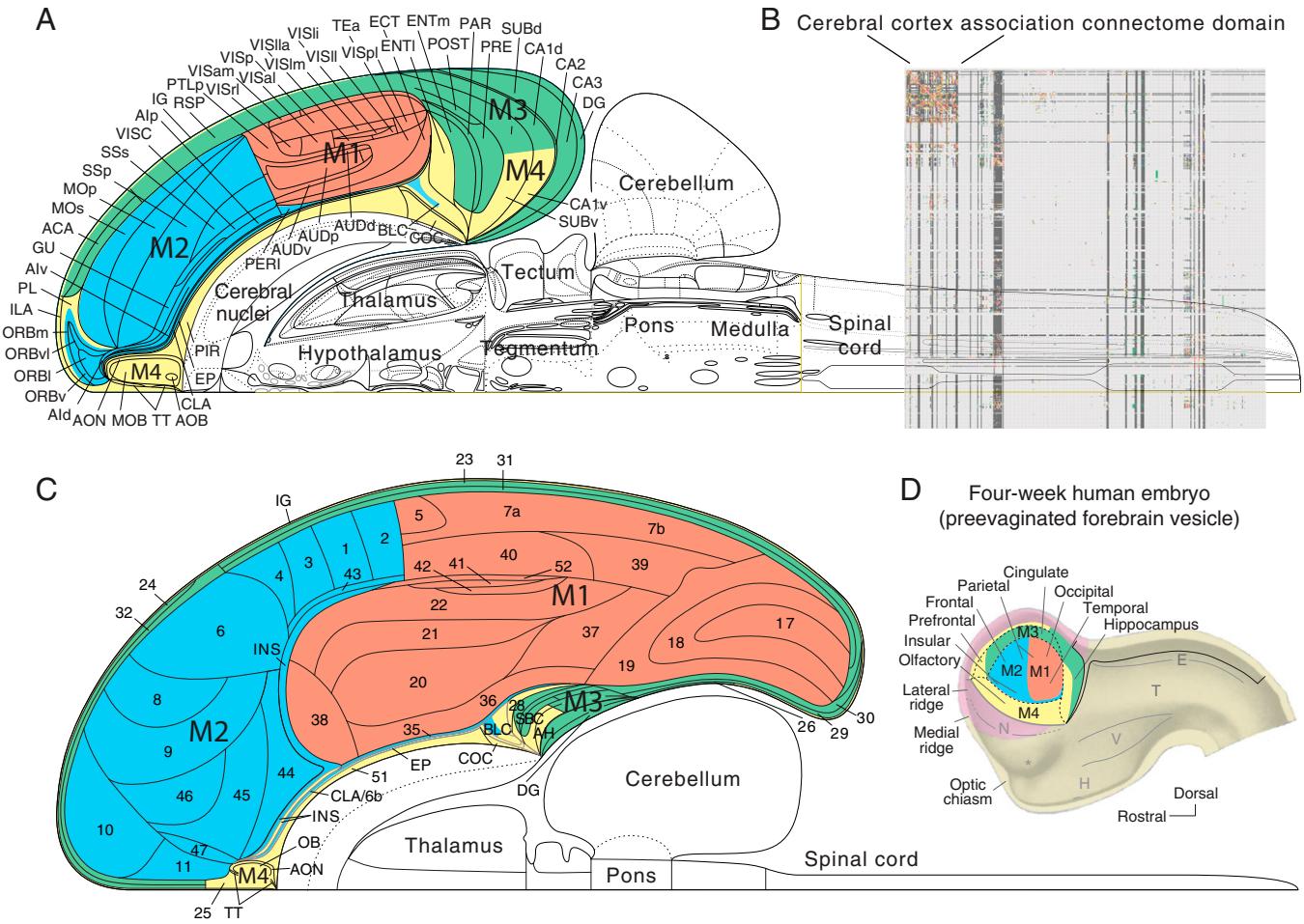

Fig. 4. Spatial distribution of cortical association modules. (*A*) Modules (M1–M4) in Figs. 2 and 3 plotted on a flatmap of right half of rat central nervous system (16); M1, red; M2, blue, M3, green, M4, yellow. See ref. 16 for high-resolution details. (*B*) The cortical association connectome (Fig. 1) shown in the context of the complete rat central nervous system connectome that has just 15% matrix coverage (fill ratio) because most literature outside the cortical association domain is not yet expertly curated (44). Abbreviations are in Fig. S2. (*C*) Histologically defined human cortical regions corresponding to rat cortical regions (correspondence documented in Fig. S2) plotted on a flatmap (45) and color coded as in *A*. AH, Ammon's horn; AON, anterior olfactory nucleus; BLC, basolateral amygdalar complex; CLA/6B, claustrum/layer 6b; COC, cortical amygdalar complex; DG, dentate gyrus; EP, entopeduncular nucleus; INS, insular region; OB, olfactory bulb; TT, tenia tecta; SBC, subicular complex. Numbers correspond to Brodmann's areas (Fig. S2). (*D*) Predicted fate map of major cerebral cortical regions with general location of rat M1–M4 (color coded as in *A* and *C*); illustrated on the right embryonic forebrain vesicle viewed from medial aspect (4-wk human; equivalent to 11-d rat, 9/10-d mouse); adapted from ref. 46. E, epithalamus; H, hypothalamus; N, cerebral nuclei; T, dorsal thalamus; V, ventral thalamus.

more centrally connected within the network, corresponding to so-called network hubs (20, 21). We identified the hubs in the cortical association network by computing four centrality measures (Fig. S1*C*) and ranking nodes according to their aggregate centrality score (Fig. S2, red cortical regions). The set with the highest scores (a value of 4, indicating high rankings across all four measures) comprised three nodes: ectorhinal, perirhinal, and lateral entorhinal areas. Interestingly, these three hubs form a topographically continuous patch of cortex that is also highly mutually connected (see discussion of rich club below). In humans, this patch generally shows the earliest, most severe pathological changes in Alzheimer's disease (22) and is implicated in temporal lobe epilepsy (23).

Another significant aspect of network organization is the presence of a "rich club," defined as a set of highly connected nodes (regions) that are also densely connected with each other (24, 25). Rich-club analysis (Fig. S3 *A* and *B*) revealed three innermost-circle rich-club nodes (lateral entorhinal area, medial entorhinal area, and claustrum) positioned within a set of 15 rich-club nodes with the greatest statistical significance (adjusted $P = 1.02 \times 10^{-11}$; false discovery rate set to 0.001). These 15 nodes are distributed within all four modules, with the greatest participation in the ventral limbic module, M4. Anatomical analysis by inspection of the reference atlas (16) readily shows that all but one (field CA1v) of these rich-club nodes form a topographically continuous U-shaped band that can be divided into a caudodorsal cortical plate pole (P1), a rostrodorsal cortical plate pole (P2), and between them a ventral cortical subplate pole (P3). The three highest-ranked hubs form a patch in P3 (Fig. S3*C*), and the lateral entorhinal area is the only cortical region that is both one of these three hubs and one of the three innermost circles of rich-club nodes. The lateral entorhinal area forms the richest set of association connections of any cerebral cortical region in rat (26).

Connection Patterns. Analysis of global major connection weight patterns between all network nodes yielded statistically significant asymmetries (Fig. S1 *D* and *E*) indicating overrepresentation and underrepresentation of weight class combinations in bidirectional connections between region pairs ($P < 0.0014$) and

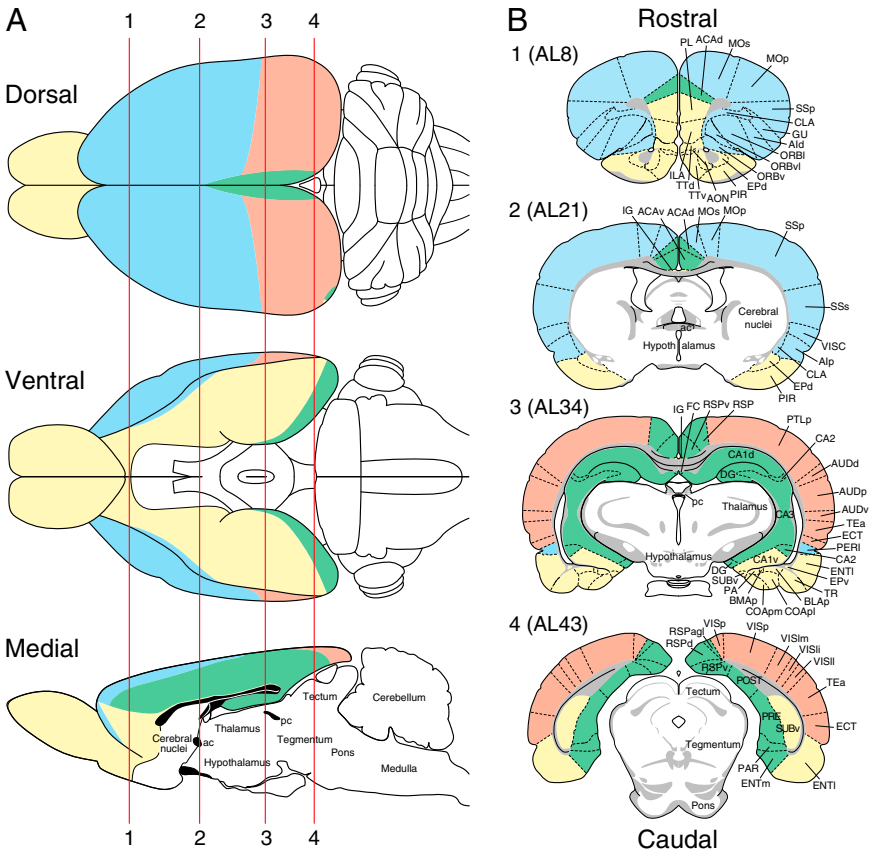

Fig. 5. Module distribution on surface and transverse views. (*A*) Surface views of the rat brain with four RCAM module domains color coded as in Figs. 3 and 4. Four vertical red lines indicate transverse levels through the brain shown in *B*. (*B*) Four transverse levels through the rat brain with modules color coded as in *A*; specifically, Atlas levels (AL) 8, 21, 34, and 43 of ref. 16 are shown. ac, anterior commissure; pc, posterior commissure; all other abbreviations are in Fig. S2.

showing that highly asymmetric weight combinations between two such nodes are less frequently encountered in the empirical connection matrix than expected if weights are randomly assigned to existing connections. This result implies at least partly "hard-wired," genetically determined biases in information flow through the cortical association macroconnectome network.

The implications of these results for connection patterns within and between modules were then assessed because all but

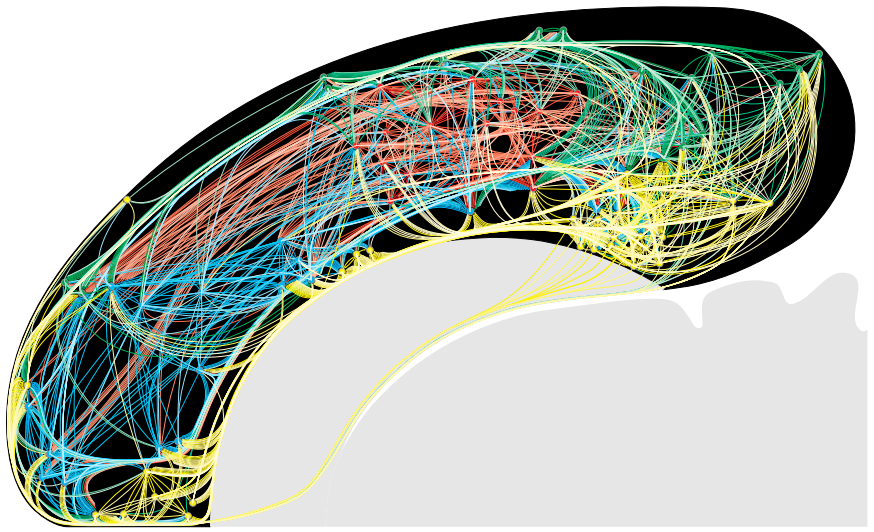

Fig. 6. All 1,923 RCAMs mapped onto the flatmap and color coded as in Figs. 3 and 4. Connection routes were placed to follow known white-matter tracts (16) and/or to follow the shortest path between origin and termination nodes (circles), without crossing unrelated nodes between them, for clarity. For a high-resolution view with labeled nodes, see Fig. S4.

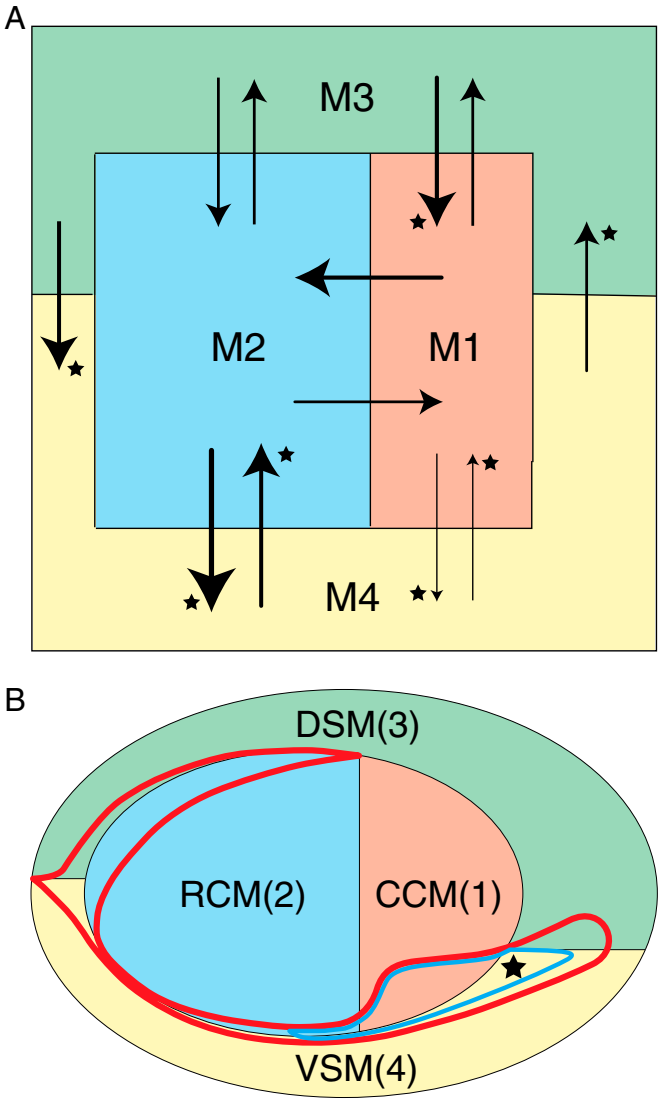

Fig. 7. Basic logic of cortical association module organization. (*A*) Schematic diagram of topological relationships between cortical association modules M1–M4 (color-coded as in Figs. 4 and 5 and abstracted from the patterns in Fig. 4 and Fig. S3) with aggregate connection weights between them. Weight estimates are based on total connection number, scaled from 1 to 5 (indicated by line thickness); statistically significant differences (Table S3) are starred. (*B*) An alternate schematic view of topological relationship between modules M1–M4, rich-club regions (within thick red outline), and three highest ranked hubs (within thinner blue line with star, which indicates the most connected node of all, the lateral entorhinal area) nested in rich-club territory. The rich club and hubs are shown on the flatmap in Fig. S3C. CCM, caudal core module (M1, red); DSM, dorsal shell module (M3, green); RCM, rostral core module (M2, blue); VSM, ventral shell module (M4, yellow).

two cortical regions (anterior olfactory nucleus and indusium griseum in M4) also connect with other modules (Fig. 2). Connection weight distribution analysis within and across modules M1–M4 revealed 894 intermodular association connections, together establishing bidirectional connections between each of the four modules (Fig. 7*A* and Tables S1 and S2). Overall, ranked qualitative estimates of connection weight indicate asymmetries in intermodular bidirectional communication, again implying at least partly hardwired biases in information flow through the RCAM network, at the level of modules.

As expected (Fig. 2), intramodular connections tend to be strong, whereas intermodular connections tend to be moderate at best (Tables S1 and S2). Furthermore, the distribution of major unidirectional (Fig. 7*A* and Tables S1–S3) connections within and between modules also indicates that each module has a unique, statistically significant pattern of association connections.

Sets of cortical association outputs and inputs between the three rich-club poles differ, and asymmetries are related to connection weight categories (Tables S4 and S5). Two organization features are obvious: major connections between the three poles are asymmetric and all share the same orientation, whereas medium-weight connections all share the opposite orientation; and between sets of poles only two of the three connection weights share the same orientation. Clearly, information flow is heavily biased at this third level of analysis, in the network formed between the three rich-club poles.

Module Configuration and Data Coverage. A critical question in statistical network analysis based on empirical data is: What minimum matrix coverage ("fill ratio") is required for stable overall patterns to emerge? This question was examined in two ways for our data. First, during curation, nine sequential versions were saved of the RCAM matrix, with coverage from 22% to 81%. Visual inspection showed that module number and composition depended on coverage, with a stable pattern emerging after 65% coverage was achieved (Fig. 8*A*). Second, module configuration stability as a function of matrix coverage was tested by performing random deletion of connectional data (Fig. 8 *B* and *C*). The median number of modules (100 random deletions) approached four and then stabilized at ∼60% coverage, confirming a minimum coverage of approximately two-thirds for qualitatively stable patterns. In our dataset, final coverage for all intermodular and intramodular connection subsets ranged from 72% to 93% (Table S6).

Bridge to Human Cortical Connectome. A highly desirable goal is to leverage detailed systems neuroscience data from animals to better understand mechanisms generating cognition in humans, where currently experimental circuit analysis faces major obstacles. For example, experimental animal histological analysis of circuitry operates at the nanometer to micrometer level for subcellular and cellular resolution, whereas human imaging methods operate at the millimeter level for gross anatomical resolution. To stimulate interactions between basic animal research and translational human connectome research, the anatomical distribution of association macroconnection modules, hubs, and rich-club members in rat were mapped onto proposed equivalents in human cortex (Fig. 4*C* and Fig. S3*D*), based on the preponderance of current evidence about the relationship between cortical parcellation in rat and human (Fig. S2).

The underlying rationale for this approach goes back to Brodmann (27), who examined >60 species representing seven orders and hypothesized that there is a basic mammalian plan of cortical structural regionalization that, like the overall body plan, is differentiated in different species. This generalization has been broadly confirmed, so it is reasonable to hypothesize that synaptic connectional data gathered in nonhuman mammals—like rodents (Figs. 1 and 2) and monkeys (28)—can be used to help interpret and propose testable hypotheses about cerebral cortical biological mechanisms in humans (at least at the macroconnection level), where almost no such data exists or is even possible with current MRI technology as discussed above.

Discussion

Our results provide an alternative to the traditional approach of describing the most general level of cerebral cortex organization—even in rodents—with reference to "lobes" named arbitrarily for overlying bones and to linear streams of connections identified by selective functional analysis. Systematic, data-driven, network analysis of the rat cortical association connectome instead reveals

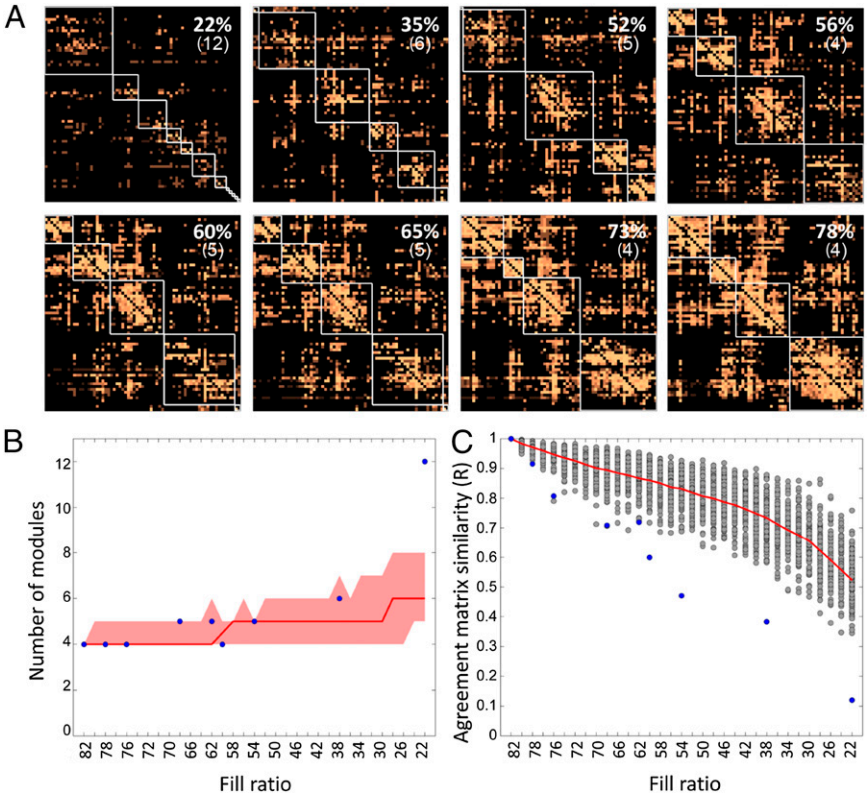

Fig. 8. Data coverage effect on final connectome pattern. (*A*) Eight versions of cortical association connectome saved during curation with indicated percent coverage (fill ratio) and number of modules (in parentheses). Matrices are based on 69 regions because the total increased to 73 during the process of curation. (*B*) Empirical matrix module number (blue point at 81% coverage), eight less-covered matrices (remaining eight blue points), median module number for randomly degraded matrices (solid red line) with corresponding minimum (red shaded area lower bound) and maximum (red shaded area upper bound). (*C*) Agreement matrix similarities between empirical matrix (81% coverage) and eight incompletely covered matrices (blue points) and randomly degraded matrices (gray points), expressed as Pearson correlation of upper matrix triangles.

novel design features (Fig. 7*B*). Based on its association connections, the entire rat cerebral cortex (*i*) is divided into four topographically and topologically nonoverlapping modules with a core–shell organization, (*ii*) has a topographically continuous rich club of regions/nodes with three poles that together span restricted parts of all four modules, and (*iii*) has its three highest ranked hubs clustered together within the caudal rich-club pole. Furthermore, each of the 73 cortical regions has a unique set of input and output association connections, and each of the four modules has a unique pattern of intramodular and intermodular connections—a unique connectional identity that overall tends to minimize connection lengths. Finally, each rich-club pole has a unique pattern of asymmetrical input and output connections with the other two poles.

The four association connection modules may thus form basic morphological units of the rat cerebral cortex. This possibility is strengthened by their predicted general localization in the earliest recognizable stage of cortical embryonic development (Fig. 4*D*). Molecular genetic mechanisms generating this regionalization and wiring pattern remain to be clarified.

The analysis strategy developed here provides a framework for going on to determine the complete cortical mesoconnectome (at the neuron-type level) and then microconnectome (at the individual neuron level) in rodents and to establish in various species the general plan of mammalian cortical organization and its differentiable features, which would include commissural connections as well as extrinsic inputs and outputs.

More globally, the structural microconnectome of nematode worms began more than a century ago (29) with light microscopy and is the only generally completed effort thus far (30). More limited analyses in mammals have usually focused on isocortical regions of the cortical plate rather than the entire cortical mantle as here. Metaanalyses revealed four structure–function modules (visual, auditory, somatomotor, fronto-limbic) in cat (31, 32) and five modules quite different from those identified here in macaque, although some striking similarities in hub and rich-club members were identified (33). Discrepancies with results presented here may be due to a combination of factors, including differences in species, nomenclature, connection weight scaling, statistical methods, and dataset completeness. Results from two recent mouse studies (34, 35) differed from those presented here, primarily due to less robust connection weight scaling, different network analysis methods, and much lower degree of matrix coverage (Table S7 and Fig. 8).

Our results encourage completion of the rodent central nervous system connectome at the same level of data accuracy and reliability, and of network analysis, displayed for the cerebral cortex (Fig. 2). The current level of curation in our knowledge management system is shown in Fig. 4*B*, suggesting a systematic curation strategy for the 10 basic topographic divisions of the central nervous system (36, 37), starting most productively with the cerebral cortex (38) and then progressing caudally through the cerebral nuclei, thalamus, hypothalamus, tectum, tegmentum, pons, cerebellum, medulla, and spinal cord (Figs. 4*A* and 5*A*, medial). A complete rat connectome involves a matrix of 503 gray matter regions with 252,506 elements (macroconnections) on each side of the central nervous system (16). Even this comprehensive matrix of macroconnections would be incomplete. At the macroscale, a complete structure–function neurome would also include peripheral ganglia and the muscles, glands, and other

body parts innervated. As microscale connectome maps continue to expand (39), a final point of convergence may be a nested multiscale "zoomable" map (12, 13) of a mammalian nervous system that reveals nonrandom network attributes of local neural circuitry as well as large-scale nervous system structure–function subsystems.

The global cortical association connectome presented here is for the presumably "normal" adult albino rat, and similar data are being generated for adult mouse (34, 35). It is now technically possible to construct similar connectomes in rodent models of disease where cortical connectopathies (39) are hypothesized, and it will be important to develop effective statistical methods for testing these hypotheses by comparing connectomes at the cellular (micrometer) and synaptic (nanometer) levels for a particular species—an approach already being applied successfully at the regional (millimeter) level for human imaging studies (40). It will be even more challenging to develop rigorous comparisons of connectomes between species, where the difficult problem of establishing homologies like those proposed here between rodent and human cortical regionalization (Fig. S2) is fundamental (41). However, developments along these lines could eventually lead to connectome-scale association studies at multiple scales of resolution and even involving multiple species—similar in principle to genome-scale association studies (42) and perhaps even correlated with them as a powerful new approach to the classification, etiology, and treatment of connectopathies underlying mental health disease.

Materials and Methods

Methods for the underlying analysis are described in detail in *SI Materials and Methods*. Briefly, data were curated for the entire cerebral cortical mantle, including both isocortex (neocortex) and allocortex (paleocortex and archicortex), and thus including all regions associated with the cortical plate and underlying cortical subplate (16). All relevant data in the primary literature were interpreted in the only available standard, hierarchically organized, annotated nomenclature for the rat (16) and compiled with supporting metadata in BAMS (brancusi.usc.edu; refs. 8, 43, and 44) by using descriptive nomenclature defined in the Foundational Model of Connectivity (12, 13). Cortical association connection reports in BAMS were encoded with ranked qualitative connection weights based on pathway tracing methodology, injection site location and extent, and anatomical density. Network analysis for modularity, small world organization, hubs, and rich club followed standard procedures described in refs. 18 and 19.

1. Kandel ER, Hudspeth AJ (2013) The brain and behavior. *Principles of Neural Science*, eds Kandel ER, Schwartz JH, Jessell TM, Siegelbaum SA, Hudspeth AJ (McGraw-Hill, New York), 5th Ed, pp 5–20.
2. Swanson LW (2012) *Brain Architecture: Understanding the Basic Plan* (Oxford Univ Press, Oxford), 2nd Ed.
3. Catani M, Mesulam M (2008) What is a disconnection syndrome? *Cortex* 44(8): 911–913.
4. Nieuwenhuys R, Voogd J, van Huijzen C (2008) *The Human Central Nervous System* (Springer, Berlin), 4th Ed.
5. Bota M, Dong H-W, Swanson LW (2003) From gene networks to brain networks. *Nat Neurosci* 6(8):795–799.
6. Sporns O, Tononi G, Kötter R (2005) The human connectome: A structural description of the human brain. *PLOS Comput Biol* 1(4):e42.
7. Bohland JW, et al. (2009) A proposal for a coordinated effort for the determination of brainwide neuroanatomical connectivity in model organisms at a mesoscopic scale. *PLOS Comput Biol* 5(3):e1000334.
8. Bota M, Dong H-W, Swanson LW (2005) Brain architecture management system. *Neuroinformatics* 3(1):15–48.
9. von Economo C (1926) Ein koeffizient für die organisationshöhle der grosshirnrinde. *Klin Wochenschr* 5:593–595.
10. Karlsen AS, Pakkenberg B (2011) Total numbers of neurons and glial cells in cortex and basal ganglia of aged brains with Down syndrome—a stereological study. *Cereb Cortex* 21(11):2519–2524.
11. Ribeiro PF, et al. (2013) The human cerebral cortex is neither one nor many: Neuronal distribution reveals two quantitatively different zones in the gray matter, three in the white matter, and explains local variations in cortical folding. *Front Neuroanat* 7:28.
12. Swanson LW, Bota M (2010) Foundational model of structural connectivity in the nervous system with a schema for wiring diagrams, connectome, and basic plan architecture. *Proc Natl Acad Sci USA* 107(48):20610–20617.
13. Brown RA, Swanson LW (2013) Neural systems language: A formal modeling language for the systematic description, unambiguous communication, and automated digital curation of neural connectivity. *J Comp Neurol* 521(13):2889–2906.
14. Bota M, Swanson LW (2007) The neuron classification problem. *Brain Res Brain Res Rev* 56(1):79–88.
15. Meynert T (1867–1868) Der bau der Gross-Hirnrinde und seine örtlichen verschiedenheiten, nebst einem pathologisch-anatomischen corollarium. *Vierteljarsschr Psychiat* 1:77–93. 198–217 (1867), 2:88–113 (1868).
16. Swanson LW (2004) *Brain Maps: Structure of the Rat Brain. A Laboratory Guide with Printed and Electronic Templates for Data, Models and Schematics* (Elsevier, Amsterdam), 3rd Ed.
17. Bota M, Talpalaru S, Hintiryan H, Dong H-W, Swanson LW (2014) BAMS2 workspace: A comprehensive and versatile neuroinformatic platform for collating and processing neuroanatomical connections. *J Comp Neurol* 522(14):3160–3176.
18. Rubinov M, Sporns O (2010) Complex network measures of brain connectivity: Uses and interpretations. *Neuroimage* 52(3):1059–1069.
19. Watts DJ, Strogatz SH (1998) Collective dynamics of 'small-world' networks. *Nature* 393(6684):440–442.
20. Sporns O, Honey CJ, Kötter R (2007) Identification and classification of hubs in brain networks. *PLoS ONE* 2(10):e1049.
21. van den Heuvel MP, Sporns O (2013) Network hubs in the human brain. *Trends Cogn Sci* 17(12):683–696.
22. Braak H, Rüb U, Schultz C, Del Tredici K (2006) Vulnerability of cortical neurons to Alzheimer's and Parkinson's diseases. *J Alzheimers Dis* 9(3, Suppl):35–44.
23. de Curtis M, Paré D (2004) The rhinal cortices: A wall of inhibition between the neocortex and the hippocampus. *Prog Neurobiol* 74(2):101–110.
24. Colizza V, Flammini A, Serrano MA, Vespignani A (2006) Detecting rich-club ordering in complex networks. *Nat Phys* 2:110–115.
25. van den Heuvel MP, Sporns O (2011) Rich-club organization of the human connectome. *J Neurosci* 31(44):15775–15786.
26. Swanson LW, Köhler C (1986) Anatomical evidence for direct projections from the entorhinal area to the entire cortical mantle in the rat. *J Neurosci* 6(10):3010–3023.
27. Brodmann K (2006) *Brodmann's Localization in the Cerebral Cortex: The Principles of Comparative Localisation in the Cerebral Cortex Based on the Cytoarchitectonics*; trans Garey L (Springer, New York).
28. Bakker R, Wachtler T, Diesmann M (2012) CoCoMac 2.0 and the future of tract-tracing databases. *Front Neuroinform* 6:30.
29. Goldschmidt R (1909) Das nervensystem von *Ascaris lumbricoides* und *megalocephala*. III. *Z Wiss Zool* 92:306–357.
30. Jarrell TA, et al. (2012) The connectome of a decision-making neural network. *Science* 337(6093):437–444.
31. Scannell JW, Blakemore C, Young MP (1995) Analysis of connectivity in the cat cerebral cortex. *J Neurosci* 15(2):1463–1483.
32. de Reus MA, van den Heuvel MP (2013) Rich club organization and intermodule communication in the cat connectome. *J Neurosci* 33(32):12929–12939.
33. Harriger L, van den Heuvel MP, Sporns O (2012) Rich club organization of macaque cerebral cortex and its role in network communication. *PLoS ONE* 7(9):e46497.
34. Zingg B, et al. (2014) Neural networks of the mouse neocortex. *Cell* 156(5):1096–1111.
35. Oh SW, et al. (2014) A mesoscale connectome of the mouse brain. *Nature* 508(7495): 207–214.
36. Nauta WJH, Feirtag M (1986) *Fundamental Neuroanatomy* (Freeman, New York).
37. Swanson LW (2000) What is the brain? *Trends Neurosci* 23(11):519–527.
38. Swanson LW (2005) Anatomy of the soul as reflected in the cerebral hemispheres: Neural circuits underlying voluntary control of basic motivated behaviors. *J Comp Neurol* 493(1):122–131.
39. Lichtman JW, Sanes JR (2008) Ome sweet ome: What can the genome tell us about the connectome? *Curr Opin Neurobiol* 18(3):346–353.
40. Zalesky A, Cocchi L, Fornito A, Murray MM, Bullmore E (2012) Connectivity differences in brain networks. *Neuroimage* 60(2):1055–1062.
41. Bota M, Arbib MA (2004) Integrating databases and expert systems for the analysis of brain structures: Connections, similarities, and homologies. *Neuroinformatics* 2(1): 19–58.
42. McCarroll SA, Feng G, Hyman SE (2014) Genome-scale neurogenetics: Methodology and meaning. *Nat Neurosci* 17(6):756–763.
43. Bota M, Swanson LW (2010) Collating and curating neuroanatomical nomenclatures: Principles and use of the Brain Architecture Knowledge Management System (BAMS). *Front Neuroinform* 4:3.
44. Bota M, Dong H-W, Swanson LW (2012) Combining collation and annotation efforts toward completion of the rat and mouse connectomes in BAMS. *Front Neuroinform* 6:2.
45. Swanson LW (1995) Mapping the human brain: past, present, and future. *Trends Neurosci* 18(11):471–474.
46. Swanson LW (2000) Cerebral hemisphere regulation of motivated behavior. *Brain Res* 886(1–2):113–164.